Environ. Sci. Technol. **2007**, *41,* 6129−6136

Oligomers in the Early Stage of Biogenic Secondary Organic Aerosol Formation and Growth

KATHERINE J. HEATON,
MATTHEW A. DREYFUS,
SHENYI WANG, AND
MURRAY V. JOHNSTON*

Department of Chemistry and Biochemistry, University of Delaware, Newark, Delaware 19716

The formation of secondary organic aerosol (SOA) by reaction of ozone with monoterpenes (β-pinene, Δ^3-carene, limonene, and sabinene) was studied on a short time scale of 3−22 s with a flow tube reactor. Online chemical analysis was performed with the Photoionization Aerosol Mass Spectrometer (PIAMS) to obtain molecular composition and the Nanoaerosol Mass Spectrometer (NAMS) to obtain elemental composition. Molecular composition data showed that dimers and higher order oligomers are formed within seconds after the onset of reaction, indicating that there is no intrinsic kinetic barrier to oligomer formation. Because oligomer formation is fast, it is unlikely that a large number of steps are involved in their formation. Therefore, ion distributions in the PIAMS spectra were interpreted through reactions of intermediates postulated in previous studies with monomer end products or other intermediates. Based on ion signal intensities in the mass spectra, organic peroxides appear to comprise a greater fraction of the aerosol than secondary ozonides. This conclusion is supported by elemental composition data from NAMS that gave C:O ratios in the 2.2−2.7 range.

Introduction

The formation of secondary organic aerosol (SOA) from volatile organic compounds (VOC) in the atmosphere is important owing to potential impacts on human health and global climate (*1*, *2*). Current models underestimate the production of SOA by as much as 1−2 orders of magnitude, highlighting the need to better understand the chemical and physical processes involved (*3*−*5*). A main contributor to SOA is the oxidation of biogenic VOC such as monoterpenes to generate products that have lower vapor pressures than the precursor molecules (*6*). In this work, SOA formation by reaction of monoterpenes with ozone is considered. The initial steps of ozonolysis are well understood in which ozone adds across the double bond to form a primary ozonide, which then decomposes into the excited Criegee intermediate (*7*). The excited Criegee intermediate can follow either the Stabilized Criegee Intermediate (SCI) Channel or the Hydroperoxy (HP) Channel to generate SOA (*8*). In the SCI channel, the excited Criegee intermediate is thermally stabilized through collisions with air. In the HP channel, the excited Criegee intermediate isomerizes to a hydroperoxide. Figure 1 shows the two pathways (R1 and R2) for β-pinene ozonolysis and examples of stable molecule end products.

SOA is produced when gas-particle partitioning of the products favors the particle phase. Efficient partitioning requires a vapor pressure on the order of 10^{-5} Torr depending on experimental conditions. New particle formation requires a much lower vapor pressure because the aerosol mass concentration and particle diameter are small at the onset of SOA production. Partitioning to the particle phase scales with aerosol mass, while the radius of curvature (Kelvin effect) strongly influences vapor pressure in the nanoparticle size range. For monoterpene ozonolysis, it was originally suggested that dicarboxylic acids, such as *cis*-pinic acid produced in α- and β-pinene ozonolysis, are precursors to particle nucleation since they are relatively nonvolatile (*9*, *10*). While these compounds have low enough vapor pressures to partition to an existing particle phase, it has been argued that the vapor pressures are still too high to form new particles (*11*, *12*). Dimers formed between an intermediate, such as a hydroperoxide or the stabilized Criegee intermediate, and a second species (either a stable molecule end product or another intermediate) seem to be better candidates for nucleating precursors (*12*, *13*).

Dimers and higher molecular weight oligomers, often referred to as humiclike substances (HULIS) because of their similar chemical properties, have been detected in laboratory generated SOA from monoterpenes (*12*, *14*−33). In these experiments, oligomers are found in the particle phase within about an hour after the onset of reaction. This time period is the shortest that can be accessed easily by the offline analytical techniques used for oligomer characterization. As the reaction time increases, the molecular weight distribution of oligomers does not increase substantially, but chemical aging is evident (*33*). Over a time period of 10+ h, infrared and mass spectrometry measurements show that the oxidized functional group content increases; volatility tandem differential mobility analyzer measurements show that the oligomer mass fraction increases, while the absolute mass of SOA does not (*33*−*36*). These observations suggest that oligomer *transformation* reactions associated with chemical aging over a period of hours may be different from oligomer *formation* reactions over a shorter time period during the early stage of SOA growth.

Recently, our group has used a photoionization aerosol mass spectrometer (PIAMS) to perform online oligomer analysis of SOA from α-pinene ozonolysis (*15*). Online analysis allows shorter time periods to be studied than offline techniques. There has been some discussion about whether the SCI or the HP channel dominates the initial stage of particle formation (*12*, *16*, *37*). Our previous work with α-pinene provides evidence for both channels, although the relative importance of each is not known (*15*). Here we extend this work to include SOA formed by ozonolysis of other monoterpenes including β-pinene, Δ^3-carene, limonene, and sabinene. The results provide additional insight into the early stage of reaction.

Experimental Section

Flow Tube Reactor. The flow tube reactor used in these experiments has been described previously (*15*, *38*). Monoterpene vapor was created by passing clean, dry air (RH<5%) over the monoterpene liquid. It was then introduced into a concentric flow tube reactor through a central injector. Ozone was generated and analyzed using a Model 49C O_3 Analyzer (Thermo Electron Corp.) and then introduced into the reactor through the outer tube. The ozone and the monoterpene vapor were mixed under laminar flow conditions. The length of the reaction chamber could be altered to allow the reaction to occur from a minimum of 3 s to a maximum of 22 s. Table 1 summarizes the experimental conditions. For β-pinene,

* Corresponding author phone: (302)831-8014; fax: (302)831-6335; e-mail mvj@udel.edu..

10.1021/es070314n CCC: $37.00 © 2007 American Chemical Society
Published on Web 08/02/2007

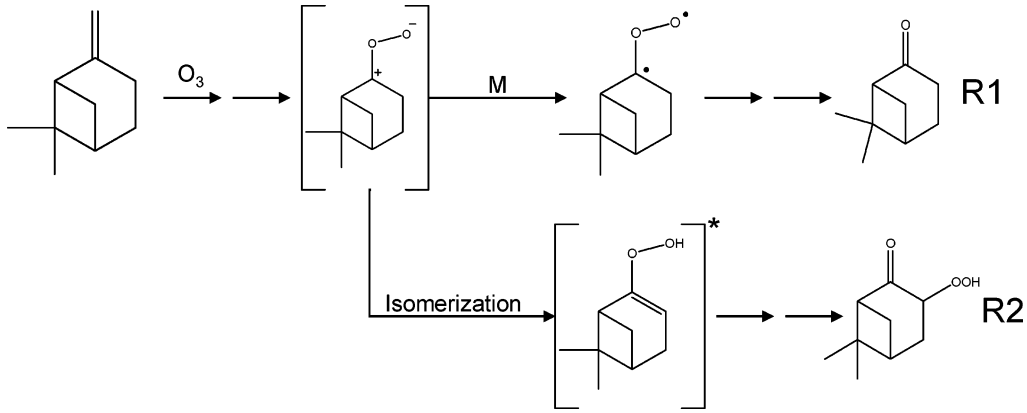

FIGURE 1. Reactions of β-pinene with ozone through the SCI channel (R1) and the HP channel (R2). Examples of monomer end products are shown for each.

TABLE 1. Summary of Experimental Conditions[a]

monoterpene	time (s)	monoterpene concn (ppm)[b]	d_m[c] (nm)	σ_g	no. concn (#/cm^3)	mass concn (μg/m^3)
β-pinene	8	55	21	1.4	6.09E+06	43
	22		29	1.3	6.08E+06	106
Δ^3-carene	3	47	24	1.3	6.86E+06	51
	22		41	1.3	6.71E+06	302
limonene	3	41	23	1.4	6.75E+06	58
	22		46	1.3	8.08E+06	561
sabinene	3	72	19	1.4	6.56E+06	35
	22		42	1.3	6.71E+06	336

[a] Ozone concentration was 1 ppm. [b] Monoterpene concentration was based on a saturated vapor; true concentrations are likely to be a half to a third of these values. [c] d_m is the mobility diameter.

the minimum reaction time had to be increased to 8 s due to the lack of particle formation at an earlier time. This is not unexpected as the ozonolysis reaction rate for β-pinene is lower than that of the other monoterpenes (*8*). As shown in Table 1, increasing the reaction time increased the mean particle diameter, number concentration, and mass concentration.

Direct analysis of the monoterpene vapors could not be done with our experimental setup; therefore, the initial concentration of each monoterpene was estimated from previously determined vapor pressures at 25 °C (*39*) assuming that a saturated vapor was produced. However, this condition is unlikely, and the monoterpene concentrations in Table 1 represent upper limits. The true concentrations are likely to be one-half to one-third of these values based on previous work by Lee and Kamens with α-pinene (*12*).

Analysis. Online analysis was performed with two aerosol mass spectrometers and a scanning mobility particle sizer (SMPS). Molecular species in the particles were characterized with a photoionization aerosol mass spectrometer (PIAMS) (*15*, *40*). With this instrument, particles were sampled through an aerodynamic lens that was designed to efficiently transmit particles with a diameter of 30−500 nm. Particles entered the source region of the mass spectrometer where they were collected on a cold probe. The collected sample was then flash desorbed with a series of infrared laser pulses, and the plume from each desorption pulse was softly ionized with coherent vacuum ultraviolet radiation from a second laser pulse. The ions from each infrared-vuv pulse sequence were mass analyzed by time-of-flight. In these experiments, each sample was collected for 10 min before analysis, and the results from 10 samples were averaged to obtain the reported mass spectra.

The elemental compositions of individual particles were obtained with a nanoaerosol aerosol mass spectrometer (NAMS) (*15*, *41*, *42*). With this instrument, particles were transmitted into the source region through a combination of aerodynamic and electrodynamic focusing. Particles were then ablated by a high-energy laser pulse to produce positively charged atomic ions, which were analyzed by time-of-flight. Each of the reported spectra represents the average of 50 single particle spectra.

Particle number concentrations, mass concentrations, and size distributions were obtained with a nano SMPS (TSI, Inc., St. Paul, MN). Particles between 4 and 150 nm were analyzed with a 120 s scanning time and a 15 s retrace period. Since size distribution data could not be obtained at the same time as a mass spectrum was being acquired, size distribution measurements were acquired before and after mass spectral analysis and were repeated at least five times to ensure reproducibility.

Chemicals. All chemicals used were the purest that were commercially available. Sabinene was purchased from Chromadex, Inc. (Santa Ana, CA), *d*-limonene was purchased from Fisher Scientific, Inc., and all other chemicals were purchased from Sigma-Aldrich (Milwaukee, WI).

Results and Discussion

The reaction conditions given in Table 1 were chosen to produce SOA on a very short time scale with sufficient mass concentration, stability, and reproducibility for analysis. Although the concentrations exceeded atmospheric levels, they provided the ability to study oligomer formation on the time scale of less than a minute to determine whether or not a kinetic barrier exists to formation. In contrast, other studies of oligomer formation typically have required time scales on the order of hours (*9*, *14*, *16*, *18*−*24*, *27*, *28*, *30*−*32*). Ozone was the limiting reactant in this experiment. Based on previously determined rate constants for reaction with monoterpenes (*8*), the amount of ozone consumed ranged from 15 to 50% for the shorter time periods to 70% or greater for the longer time periods.

The PIAMS spectra obtained in this study show similar features to the spectra in our previous work of SOA produced from α-pinene ozonolysis (*15*). The high *m*/*z* range, above about 290 m/z, shows ions corresponding to dimers and higher order oligomers. The mid *m*/*z* range, from about 150 to 200 m/z, shows ions corresponding to monomers. Figure 2 shows the high and mid *m*/*z* ranges of the PIAMS spectra for β-pinene, Δ^3-carene, limonene, and sabinene for a reaction time of 22 s. The high *m*/*z* regions show a progression of peaks separated by 14−16 Daltons, which is typical of oligomer mass spectra taken in longer time frame experiments. As will be discussed later, the molecular masses of expected dimer products extend only to about 400 *m*/*z* depending on the specific monoterpene precursor. Since ions are observed in several cases above this *m*/*z*, it is likely that

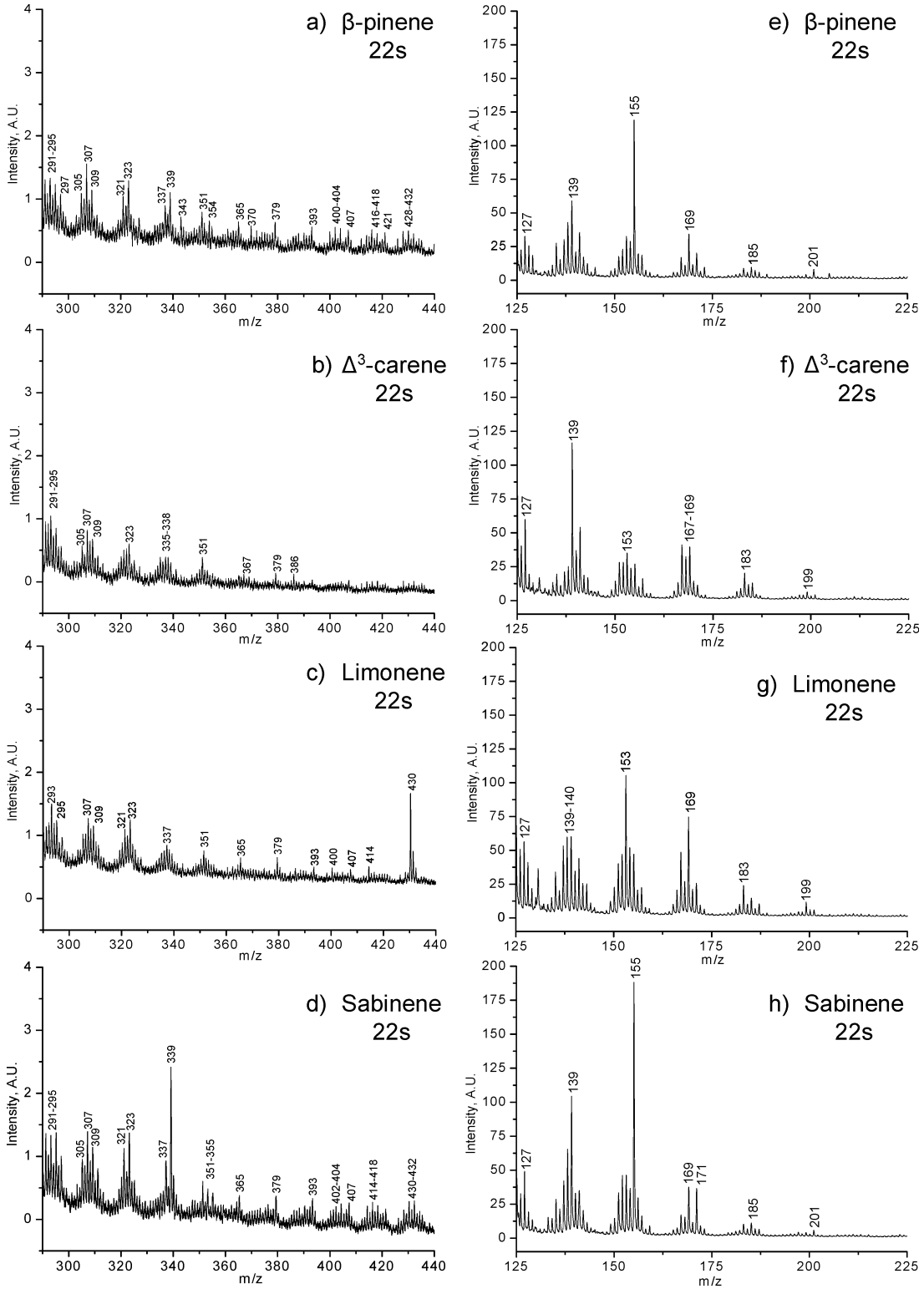

FIGURE 2. PIAMS spectra of SOA formed by monoterpene ozonolysis. Parts a−d show the high *m/z* region associated with oligomers (*m/z* 290−440), and parts e−h show the mid *m/z* region associated with monomers (*m/z* 125−225).

higher order oligomers are also being produced. Although PIAMS is able to confirm the presence of oligomers, extensive fragmentation precludes a determination of the molecular size distribution. The mid m/z region is 50−100 times more intense than the high m/z region, and the distribution of ions in the mid m/z region is similar (though not identical) for different monoterpene precursors.

Because oligomers appear very quickly after the onset of reaction, the number of steps involved in their formation is likely to be small. For this reason, we have interpreted the spectra in Figure 2 through reactions of an intermediate, either the SCI or a hydroperoxide, to produce a dimer or higher order oligomer. The intermediate could react with a monomer end product known to be produced by ozonolysis or with another intermediate. Dimers of this type previously have been suggested as the nucleating agents for SOA particle formation (*12*, *15*, *16*). Figure 3 illustrates some possible pathways for β-pinene based on this approach.

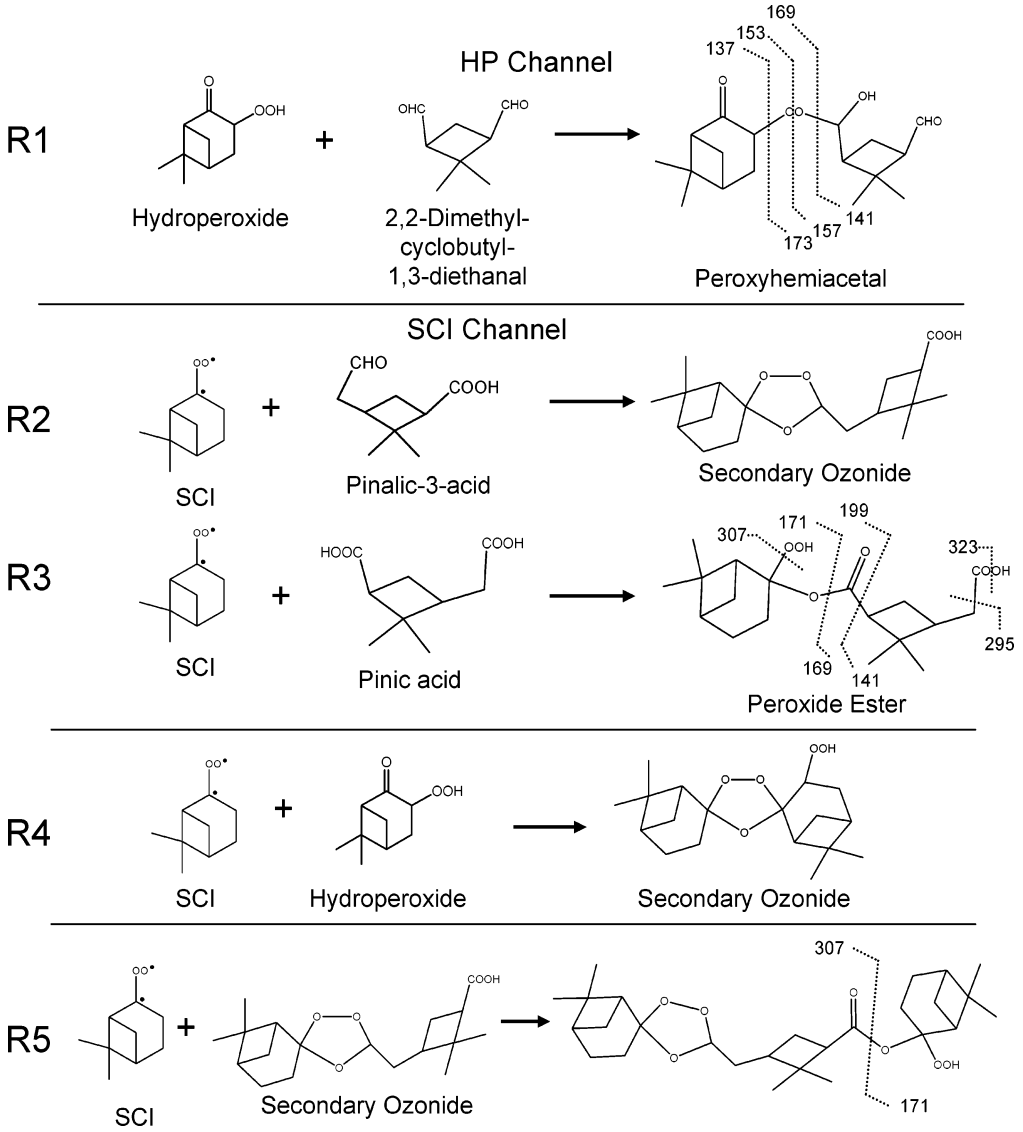

FIGURE 3. Examples of dimer formation reactions. R1−R3 show reactions of an intermediate with a monomer end product. R4 shows a reaction of two intermediates. R5 shows formation of a trimer. The dotted lines indicate possible fragmentation pathways during vaporization and ionization that could lead to ions observed in the PIAMS spectra.

R1 in Figure 3 shows the example of a hydroperoxide reacting with a monomer end product that contains a carbonyl group (2,2-dimethylcyclobutyl-1,3-diethanal) to form a peroxyhemiacetal. R2 and R3 show examples of the SCI reacting with monomer end products that contains an aldehyde (pinalic-3-acid in R2) or a carboxylic acid (pinic acid in R3) to produce a secondary ozonide or peroxide ester, respectively. R4 in Figure 3 shows an example of two intermediates reacting, in this case the SCI and a hydroperoxide containing a carbonyl to produce a secondary ozonide. R1−R4 illustrate dimer formation routes. Higher order oligomers may also form if an intermediate reacts with a dimer, which is illustrated by R5 in Figure 3 for the reaction of the SCI with a secondary ozonide. Based on reactions of these types, possible sources for the prominent ions in the PIAMS spectra were postulated for each monoterpene.

The most prominent ions in the mid and high m/z regions of Figure 2 have an odd number m/z, suggesting that they are formed by fragmentation of larger ions from the molecular reaction products. For this reason, plausible fragmentation pathways of the products must be considered. Organic peroxides and peroxide esters may break in the middle of the molecule to produce ions in the mid m/z region, as shown in R1 and R3 of Figure 3 or in the high m/z region as shown in R4. Products containing carbonyl, aldehyde, or hydroxyperoxide groups may fragment by the loss of a low mass species, and several examples are shown in R3. Typical losses include 17 (OH), 18 (H_2O), 29 (HCO), 33 (OOH), 45 (COOH), and combinations thereof.

High m/z Region. Possible dimers that could be formed during β-pinene ozonolysis are summarized for reactions of intermediates with monomer end products (Table 2) or intermediates with other intermediates (Table 3). Similar tables are given for the other monoterpenes in the Supporting Information. The intermediates include the SCI, hydroperoxides from reactions that were proposed previously for α- and β-pinene (*10*, *16*), and the hydroperoxide formed by addition of water to the SCI (the MW 172 intermediate in Tables 2 and 3). The monomer end products in these tables were identified in previous studies of monoterpene ozonolysis (*17*, *19*, *26*, *30*). For each dimer combination, the expected fragment ions are determined as described in the previous paragraph and illustrated in Figure 3. If an expected fragment ion of the dimer matches an ion in the high m/z region of the mass spectrum (Figure 2), then an "x" is entered in its position in the table. As illustrated in Tables 2 and 3 for β-pinene, most dimer combinations can be mapped to at least one ion observed in the mass spectrum.

TABLE 2. Possible Dimer Products from β-Pinene Ozonolysis That Are Formed by the Reaction of an Intermediate (Ordinate) with a Monomer End Product (Abscissa)[a,b]

β-Pinene Ozonolysis Products																	
	M.W.	MW of products	138	140	152	154		156	170		172	184	186			198	200
		Structures	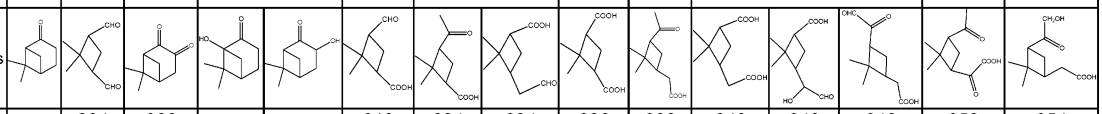														
SCI	154			294 X	306 X			310 X	324 X	324 X	326 X	338 X	340 X	340 X	340 X	352 X	354 X
Hydroperoxides	170		308 X	310 X	322 X	324 X	324 X	326 X	340 X	340 X	NR	354 X	NR	356 X	356 X	368 X	370 X
Hydroperoxides	172	*	310 X		324 X				342 X	342 X	NR	356 X	NR			370 X	372 X
Hydroperoxides	186		324 X		338 X	340 X	340 X	342 X	356 X	356 X	NR	370 X	NR	372 X	372 X	384 X	
Hydroperoxides	202		340 X	342 X	354 X	356 X	356 X		372 X	372 X	NR		NR	388 X	388 X	400 X	402 X

[a] An 'X' indicates that the dimer can be mapped to one or more prominent ions in the high *m/z* region of the PIAMS spectrum. An empty space indicates that no prominent ions could be mapped to the dimer product. [b] *This hydroperoxide is formed by reaction of the SCI with water. NR = no reaction; a dimer cannot be formed from these monomers.

TABLE 3. Possible Dimer Products from β-Pinene Ozonolysis That Are Formed by the Reaction of Two Intermediates[a,b]

β-Pinene Ozonolysis Products						
		SCI	Hydroperoxides			
MW of products	M.W	154	170	172	186	202
	Structures	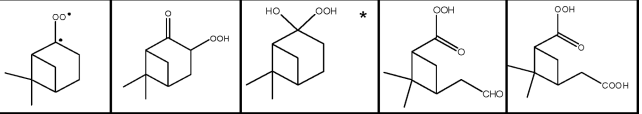				
154	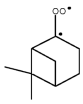					
170	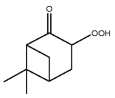	324 X	340 X			
172	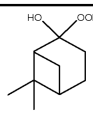 *	NR	342 X	NR		
186	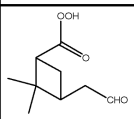	340 X	356 X	358 X	372 X	
202	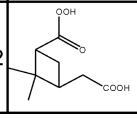	356 X	372 X	374 X	388 X	404 X

[a] An 'X' indicates that the dimer can be mapped to one or more prominent ions in the high *m/z* region of the PIAMS spectrum. An empty space indicates that no prominent ions could be mapped to the dimer product. [b] *This hydroperoxide is formed by reaction of the SCI with water. NR = no reaction; a dimer cannot be formed from these monomers.

Table 4 lists prominent ions in the high *m/z* region for each precursor. Also shown are possible reaction pathways through the SCI and HP channels that could lead to products consistent with these *m/z* values. In most cases, products from both channels can be mapped to a particular *m/z* in the spectrum. In a few cases, only one of the two channels can be mapped, and sometimes neither channel can be mapped to a particular *m/z*. The picture that emerges from this analysis is that neither the SCI nor the HP channel can be excluded as a possible source of SOA. Most ions above

TABLE 4. Summary of Prominent Ions in the High *m/z* Region of the PIAMS Spectra That Can Be Mapped to the HP or SCI Channels[a]

ions detected	HP	SCI	ions detected	HP	SCI
		β-Pinene			
291	x	x	365		
293		x	370	x	x
295	x	x	379		
297	x	x	393		
305	x	x	400	x	
307	x	x	402	x	
309	x	x	404	x	
321	x	x	407		
323	x	x	416		
337	x	x	418		
339	x	x	421		
343	x		428		
351	x	x	430		
354	x	x	432		
		Δ^3-Carene			
291			335	x	x
293			337	x	x
295		x	338	x	x
305		x	351	x	x
307		x	367	x	x
309		x	379		
323		x	386	x	x
		Limonene			
293	x		365	x	
295	x	x	379		x
307	x	x	393	x	x
309	x	x	400	x	x
321	x	x	407	x	
323	x	x	414	x	
337	x	x	430		
351	x	x			
		Sabinene			
291	x	x	355	x	x
293		x	365		
295	x	x	379		
305	x	x	393		
307	x	x	402	x	
309	x	x	404	x	
321	x	x	407		
323	x	x	414		
337	x	x	416		
339	x	x	418		
351			430		
353	x	x	432		

[a] An 'X' indicates that the channel(s) give product(s) that can be mapped to prominent ions in the PIAMS spectra.

400 m/z cannot be mapped to a dimer because the m/z exceeds the molecular masses of all possible combinations. In these cases, higher order oligomers are indicated.

Mid *m/z* Region. The mid m/z region is significantly more intense than the high m/z region. Ions observed in this region are similar to those reported by Docherty et al. using a thermal desorption electron ionization method (*16*). This similarity suggests that the chemical processes associated with SOA formation in the Docherty experiments (smog chamber, lower precursor concentrations) are similar to those associated with this work (flow tube, higher precursor concentrations). Fragment ions in this region can be mapped to both dimers and monomers. The temperature dependence of thermal desorption in the Docherty et al. experiments suggest that both types of compounds are present (*16*). As illustrated in Figure 3, dimers consisting of peroxyhemiacetals (R1) and peroxide esters (R3) would be expected to give fragment ions in the mid m/z region, while secondary ozonides (R2, R4) would not unless the fragmentation arises from a higher order oligomer (R5). It should be noted that R1 in Figure 3 is not exclusively linked to the HP channel: it is possible that the hydroperoxide produced by the addition of water to the SCI reacts in this manner to produce a dimer. For example, the hydroperoxide from the SCI of β-pinene (MW 172 intermediate in Tables 2 and 3) could react via R1 in Figure 3 to produce a dimer that subsequently fragments to give an ion at 155 m/z, which is the base peak in the β-pinene SOA spectrum in Figure 2e.

TABLE 5. C:O Atomic Ratios of Monoterpene SOA

	secondary ozonide products[a]	organic peroxides products[b]	intermediate products[c]	measured with NAMS
β-pinene	3.5	3.0	2.6	2.2
Δ^3-carene	3.1	2.7	2.5	2.3
limonene	2.9	2.5	2.4	2.2
sabinene	3.6	3.2	3.0	2.7

[a] These values are the average of all dimer products mapped to the PIAMS spectra that contain a secondary ozonide [b] These values are the average of all dimer products mapped to the PIAMS spectra that contain an organic peroxide, including both the SCI and HP channels [c] These values are the average of all dimer products mapped to the PIAMS spectra that are formed by the combination of two intermediates.

The higher intensities of mid m/z ions relative to high m/z ions suggest that most of the SOA is in the form of oligomers from hydroperoxides rather than secondary ozonides. This conclusion is supported by iodometric titrations of monoterpene SOA by Docherty et al. showing that SOA is composed primarily of organic peroxides (*16*).

Elemental Composition. Because significant fragmentation occurs when dimers and higher order oligomers are vaporized and ionized, it is helpful to characterize the aerosol by a different technique. In this study, online chemical analysis was also performed with a nanoaerosol mass spectrometer (NAMS) to give the elemental composition of individual particles. In particular, the measured C:O atomic ratios can be compared to the ratios expected for the various dimer combinations. The mass spectra of monoterpene SOA are similar to those reported previously for α-pinene (*15*), consisting of multiply charged carbon and oxygen ions. The relative intensities of these ions are combined to give the C:O atomic ratio using the method described by Wang et al. (*41*). The C:O ratios determined from these spectra are given in Table 5. Also shown are the average C:O ratios expected for three types of dimers: secondary ozonides produced from reaction of the SCI with an aldehyde (R2 in Figure 3), dimers containing an organic peroxide (R1, R3, R4 in Figure 3), and dimers formed by the reaction of an intermediate with another intermediate. These averages are determined only from the dimer combinations mapped to prominent ions in the high m/z regions, i.e., "x" entries in Tables 2 and 3. Note that only the SCI channel contributes to secondary ozonide formation, while both the SCI and HP channels can contribute to organic peroxide formation.

Table 5 shows that the organic peroxide products have C:O ratios significantly smaller than the secondary ozonide products, and the dimers formed by reaction of two intermediates have smaller C:O ratios than the complete set of organic peroxide products. The measured C:O ratios are smaller than all three types of products. Several conclusions can be drawn from this table. First, organic peroxides, particularly those that are formed by the reaction of two intermediates, are more likely components of monoterpene SOA than secondary ozonides since their C:O ratios are closer to the measured values. Second, the measured C:O ratio is somewhat dependent on monoterpene precursor. In particular, sabinene SOA has a larger C:O ratio than the others, and this is reflected by higher predicted C:O ratios of the dimer products. Third, the measured C:O ratios are uniformly lower than those of all three types of dimers. The origin of the additional oxygen is not known. It is possible that the more oxygenated intermediates contribute most to SOA formation and growth or that small molecules such as H_2O

or H_2O_2 may cocondense on the particles to decrease the effective C:O ratio.

Oligomers in SOA Formation. Online mass spectrometry provides direct evidence for dimer formation in SOA from all monoterpenes studied here (β-pinene, Δ^3-carene, limonene, and sabinene) and in our previous work (α-pinene) (*15*). In most cases, formation of higher order oligomers is also indicated. There appears to be no intrinsic kinetic barrier to this process: dimers are detected within seconds after the onset of reaction. Because dimer formation is fast, it is unlikely that a large number of steps are involved in their formation. Therefore, ion distributions in the PIAMS mass spectra were interpreted through reactions of intermediates postulated in previous studies with monomer end products or other intermediates. Based on ion signal intensities in the mass spectra, organic peroxides, particularly those formed by the reaction of two intermediates, appear to comprise a greater fraction of the aerosol than secondary ozonides. Currently, the relative contributions of the SCI and HP channels to organic peroxide formation cannot be determined. Measured C:O ratios are also more consistent with organic peroxides than secondary ozonides. However, the measured ratios are smaller than the expected ratios based on likely dimer combinations, suggesting the presence of additional reactions.

Taken together, these results strongly implicate dimers and perhaps higher order oligomers as key chemical components in the early stage of biogenic SOA formation and growth. Further elucidation of these reactions requires online analytical methods that induce less fragmentation so that molecular weight distributions and mass concentrations can be determined.

The role of dimers in new particle formation and growth is ultimately tied to vapor pressure. Several approaches have been developed to estimate vapor pressures when experimental measurements are unavailable (*43*−*47*). In this work, the SPARC online calculator (http://sparc.chem.uga.edu/sparc/) (*44*, *45*) was used to estimate vapor pressures of several of the dimer products that were postulated. The dimers investigated included the largest and smallest molecular weights and the largest and smallest calculated C:O ratios from among the possible combinations. The dimer vapor pressures were uniformly low: in each case a vapor pressure below 1×10^{-8} Torr was calculated, which is thought to be sufficient for new particle formation (*48*). Thus, the mass concentration of SOA in the early stages of particle formation and growth may be linked simply to the total concentration of all dimers formed rather than to the concentrations of specific monomer combinations.

Acknowledgments

This research was supported by grants from the National Science Foundation (CHE-0517972) and the United States Environmental Protection Agency (R829622010 and RD83-216601). Although the research described in this article was funded in part by the U.S.E.P.A., it has not been subjected to the Agency's required peer and policy review; therefore, it does not necessarily reflect the views of the Agency, and no official endorsement should be inferred.

Supporting Information Available

Fragmentation of dimer products from each monoterpene and the corresponding ions in the PIAMS mass spectra. This material is available free of charge via the Internet at http://pubs.acs.org.

Literature Cited

(1) Laden, F.; Neas, L. M.; Dockery, D. W.; Schwartz, J. Association of Fine Particulate Matter from Different Sources with Daily Mortality in Six U.S. Cities. *Environ. Health Perspect.* **2000**, *108* (10), 941−947.

(2) Kanakidou, M.; Seinfeld, J. H.; Pandis, S. N.; Barnes, I.; Dentener, F. J.; Facchini, M. C.; Van Dingenen, R.; Ervens, B.; Nenes, A.; Nielson, C. J.; Swietlicki, E.; Putaud, J. P.; Balkanski, Y.; Fuzzi, S.; Horth, J.; Moortgat, G. K.; Winterhalter, R.; Myhre, C. E. L.; Tsigaridis, K.; Vignati, E.; Stephanou, E. G.; Wilson, J. Organic aerosol and global climate modelling: a review. *Atmos. Chem. Phys.* **2005**, *5*, 1053−1123.

(3) Heald, C. L.; Jacob, D. J.; Park, R. J.; Russell, L. M.; Huebert, B. J.; Seinfeld, J. H.; Liao, H.; Weber, R. J. A large organic aerosol source in the free troposhpere missing from current models. *Geophys. Res. Lett.* **2005**, *32*, L18809, doi:10.1029/2005GL023831.

(4) de Gouw, J. A.; Middlebrook, A. M.; Warneke, C.; Goldan, P. D.; Kuster, W. C.; Roberts, J. M.; Fehsenfeld, F. C.; Worsnop, D. R.; Canagaratna, M. R.; Pszenny, A. A. P.; Keene, W. C.; Marchewka, M.; Bertman, S. B.; Bates, T. S. Budget of organic carbon in a polluted atmosphere: Results from the New England Air Quality Study in 2002. *J. Geophys. Res.* **2005**, *110* (D16305), doi:10.1029/2004JD005623.

(5) Volkamer, R.; Jimenez, J. L.; San Martini, F.; Dzepina, K.; Zhang, Q.; Salcedo, D.; Molina, L. T.; Worsnop, D. R.; Molina, M. J. Secondary organic aerosol formation from anthropogenic air pollution: Rapid and higher than expected. *Geophys. Res. Lett.* **2006**, *33* (L17811), doi:10.1029/2006GL026899.

(6) Guenther, A.; Hewitt, C. N.; Erickson, D.; Fall, R.; Geron, C.; Graedel, T.; Harley, P.; Klinger, L.; Lerdau, M.; McKay, W. A.; Pierce, T.; Scholes, B.; Steinbrecher, R.; Tallamraju, R.; Taylor, J.; Zimmerman, P. A global model of natural volatile organic compound emissions. *J. Geophys. Res.* **1995**, *100* (D5), 8873−8892.

(7) Criegee, R. Mechanism of Ozonolysis. *Angew. Chem., Int. Ed. Engl.* **1975**, *14* (11), 745−751.

(8) Calvert, J. G.; Atkinson, R.; Kerr, J. A.; Madronich, S.; Moortgat, G. K.; Wallington, T. J.; Yarwood, G. *The Mechanisms of Atmospheric Oxidation of the Alkenes*; Oxford University Press, Inc.: New York, NY, 2000; p 552.

(9) Christoffersen, T. S.; Hjorth, J.; Horie, O.; Jensen, N. R.; Kotzias, D.; Molander, L. L.; Neeb, P.; Ruppert, L.; Winterhalter, R.; Virkkula, A.; Wirtz, K.; Larsen, B. R. cis-Pinic Acid, a Possible Precursor for Organic Aerosol Formation from Ozonolysis of α-Pinene. *Atmos. Environ.* **1998**, *32* (10), 1657−1661.

(10) Jenkin, M. E.; Shallcross, D. E.; Harvey, J. N. Development and application of a possible mechanism for the generation of cis-pinic acid from the ozonolysis of α- and β-pinene. *Atmos. Environ.* **2000**, *34*, 2837−2850.

(11) Zhang, K. M.; Wexler, A. S. A hypothesis for growth of fresh atmospheric nuclei. *J. Geophys. Res.* **2002**, *107* (D21), AAC 15-1-6.

(12) Lee, S.; Kamens, R. M. Particle nucleation from the reaction of α-pinene and O_3. *Atmos. Environ.* **2005**, *39*, 6822−6832.

(13) Ziemann, P. J. Aerosol products, mechanisms, and kinetics of heterogenous reactions of ozone with oleic acid in pure and mixed particles. *Faraday Discuss.* **2005**, *130*, 469−490.

(14) Tolocka, M. P.; Jang, M.; Ginter, J. M.; Cox, F. J.; Kamens, R. M.; Johnston, M. V. Formation of Oligomers in Secondary Organic Aerosol. *Environ. Sci. Technol.* **2004**, *38* (5), 1428−1434.

(15) Tolocka, M. P.; Heaton, K. J.; Dreyfus, M. A.; Wang, S.; Zordan, C. A.; Saul, T. D.; and Johnston, M. V. The Chemistry of Particle Inception and Growth During α-Pinene Ozonolysis. *Environ. Sci. Technol.* **2006**, *40*, 1843−1848.

(16) Docherty, K. S.; Wu, W.; Lim, Y. B.; Ziemann, P. J. Contributions of Organic Peroxides to Secondary Aerosol Formed from Reaction of Monoterpenes with O_3. *Environ. Sci. Technol.* **2005**, *39* (11), 4049−4059.

(17) Warscheid, B.; Hoffman, T. Structural elucidation of monoterpene oxidation products by ion trap fragmentation using on-line atmospheric pressure chemical ionisation mass spectrometry in the negative ion mode. *Rapid Commun. Mass Spectrom.* **2001**, *15*, 2259−2272.

(18) Warscheid, B.; Hoffman, T. Direct analysis of highly oxidised organic aerosol constituents by on-line ion trap mass spectrometry in the negative-ion mode. *Rapid Commun. Mass Spectrom.* **2002**, *16*, 496−504.

(19) Yu, J.; Cocker, D. R., III; Griffin, R. J.; Flagan, R. C.; Seinfeld, J. H. Gas-Phase Ozone Oxidation of Monoterpenes: Gaseous and Particulate Products. *J. Atmos. Chem.* **1999**, *34*, 207−258.

(20) Yu, J.; Flagan, R. C.; Seinfeld, J. H. Identification of Products Containing -COOH, -OH, and -C=O in Atmospheric Oxidation of Hydrocarbons. *Environ. Sci. Technol.* **1998**, *32* (16), 2357−2370.

(21) Jang, M.; Kamens, R. M. Newly characterized products and composition of secondary aerosols from the reaction of α-pinene with ozone. *Atmos. Environ.* **1999**, *33*, 459−474.
(22) Jaoui, M.; Kamens, R. M. Mass Balance of Gaseous and Particulate Products from β-Pinene/O_3/Air in the Absence of Light and β-Pinene/NO_x/Air in the Presence of Natural Sunlight. *J. Atmos. Chem.* **2003**, *45*, 101−141.
(23) Jaoui, M.; Kamens, R. M. Gaseous and Particulate Oxidation Products Analysis of a Mixture of α-Pinene + β-Pinene/O_3/Air in the Absence of Light and α-pinene + β-pinene/NO_x/Air in the Presence of Natural Sunlight. *J. Atmos. Chem.* **2003**, *44*, 259−297.
(24) Kamens, R. M.; Jang, M.; Chien, C.-j.; Leach, K. Aerosol Formation from the Reacion of α-pinene and Ozone using a Gas-Phase Kinetics-Aerosol Partitioning Model. *Environ. Sci. Technol.* **1999**, *33*, 1430−1438.
(25) Colville, C. J.; Griffin, R. J. The roles of individual oxidants in secondary organic aerosol formation from Δ^3-carene: 1. gas-phase chemical mechanism. *Atmos. Environ.* **2004**, *38*, 4001−4012.
(26) Colville, C. J.; Griffin, R. J. The roles of individual oxidants in secondary organic aerosol formation from Δ^3-carene: 2. SOA formation and oxidant contribution. *Atmos. Environ.* **2004**, *38*, 4013−4023.
(27) Koch, S.; Winterhalter, R.; Uherek, E.; Kolloff, A.; Neeb, P.; Moortgat, G. K. Formation of new particles in the gas-phase ozonolysis of monoterpenes. *Atmos. Environ.* **2000**, *34*, 4031−4042.
(28) Winterhalter, R.; Neeb, P.; Grossmann, D.; Kolloff, A.; Horie, O.; Moortgat, G. K. Products and Mechanism of the Gas Phase Reaction of Ozone with β-pinene. *J. Atmos. Chem.* **2000**, *35* (2), 165−197.
(29) Winterhalter, R.; Van Dingenen, R.; Larsen, B. R.; Jensen, N. R.; Hjorth, J. LC-MS analysis of aerosol particles from the oxidation of α-pinene by ozone and OH-radicals. *Atmos. Chem. Phys. Discuss.* **2003**, *3*, 1−39.
(30) Leungsakul, S.; Jaoui, M.; Kamens, R. M. Kinetic Mechanism for Predicting Secondary Organic Aerosol Formation from the Reaction of d-Limonene with Ozone. *Environ. Sci. Technol.* **2005**, *39* (24), 9583−9594.
(31) Hoffman, T.; Bandur, R.; Marggraf, U.; Linscheid, M. Molecular composition of organic aerosols formed in the α-pinene/O_3 reaction: Implications for new particle formation processes. *J. Geophys. Res.* **1998**, *103* (D19), 25,569−25,578.
(32) Hoppel, W.; Fitzgerald, J.; Frick, G.; Caffrey, P. F.; Pasternack, L.; Hegg, D. A.; Gao, S.; Leaitch, R.; Shantz, N.; Cantrell, C.; Albrechcinski, T.; Ambrusko, J.; Sullivan, W. Particle formation and growth from ozonolysis of α-pinene. *J. Geophys. Res.* **2001**, *106* (D21), 27603−27,618.
(33) Kalberer, M.; Sax, M.; Samburova, V. Molecular Size Evolution of Oligomers in Organic Aerosols Collected in Urban Atmospheres and Generated in a Smog Chamber. *Environ. Sci. Technol.* **2006**, *40*, 5917−5922.
(34) Sax, M.; Zenobi, R.; Baltensperger, U.; Kalberer, M. Time resolved infrared spectroscopic analysis of aerosol formed by photo-oxidation of 1,3,5-trimethylbenzene and a-pinene. *Aerosol Sci. Technol.* **2005**, *39*, 822−830.
(35) Baltensperger, U.; Kalberer, M.; Dommen, J.; Paulsen, D.; Alfarra, R.; Coe, H.; Fisseha, R.; Gascho, A.; Gysel, M.; Nyeki, S.; Sax, M.; Steinbacher, M.; Prevot, A.; Sjogren, S.; Weingartner, E.; Zenobi, R. Secondary organic aerosols from anthropogenic and biogenic precursors. *Faraday Discuss.* **2005**, *130*, 265−278.
(36) Paulsen, D.; Weingartner, E.; Alfarra, M. R.; Baltensperger, U. Volatility measurements of photochemically and nebulizer-generated organic aerosol particles. *J. Aerosol Sci.* **2005**, *37*, 1025−1051.
(37) Bonn, B.; Schuster, G.; Moortgat, G. K. Influence of Water Vapor on the Process of New Particle Formation during Monoterpene Ozonolysis. *J. Phys. Chem. A* **2002**, *106*, 2869−2881.
(38) Tolocka, M. P.; Saul, T. D.; Johnston, M. V. Reactive Uptake of Nitric Acid into Aqueous Sodium Chloride Droplets Using Real-Time Single-Particle Mass Spectrometry. *J. Phys. Chem. A* **2004**, *108* (14), 2659−2665.
(39) Bilde, M.; Pandis, S. N. Evaporation Rates and Vapor Pressures of Individual Aerosol Species Formed in the Atmospheric Oxidation of α- and β-pinene. *Environ. Sci. Technol.* **2001**, *35* (16), 3344−3349.
(40) Oktem, B.; Tolocka, M. P.; Johnston, M. V. On-Line Analysis of Organic Componenets in Fine and Ultrafine Particles by Photoionization Aerosol Mass Spectrometry. *Anal. Chem.* **2004**, *76* (2), 253−261.
(41) Wang, S.; Zordan, C. A.; Johnston, M. V. Chemical Characterization of Individual, Airborne Sub-10-nm Particles and Molecules. *Anal. Chem.* **2006**, *78* (6), 1750−1754.
(42) Wang, S.; Johnston, M. V. Airborne Nanoparticle Characterization with a Digital Ion Trap-Reflectron Time of Flight Mass Spectrometer. *Int. J. Mass Spectrom.* **2006**, *258*, 50−57.
(43) Chattopadhyay, S.; Ziemann, P. J. Vapor Pressures of Substituted and Unsubstituted Monocarboxylic and Dicarboxylic Acids Measured Using an Imporoved Thermal Desorption Particle Beam Mass Spectrometry Method. *Aerosol Sci. Technol.* **2005**, *39*, 1085−1100.
(44) Carreira, L. A.; Hilal, S. H.; Karickhoff, S. W. Estimation of Chemical Reactivity Parameters and Physical Properties of Organic Molecules Using SPARC. In *Theoretical and Computational Chemistry, Quantitative Treatment of Solute/Solvent Interactions*; Elsevier Publishers: Amsterdam, 1994; p 368.
(45) Hilal, S. H.; Karickhoff, S. W.; Carreira, L. A. Prediction of the Vapor Pressure Boiling Point, Heat of Vaporization and Diffusion Coefficient of Organic Compounds. *QSAR Comb. Sci.* **2003**, *22*, 565−574.
(46) Makar, P. A. The Estimation of Organic Gas Vapour Pressure. *Atmos. Environ.* **2001**, *35*, 961−974.
(47) Asher, W. E.; Pankow, J. F.; Erdakos, G. B.; Seinfeld, J. H. Estimating the vapor pressures of multi-functional oxygen-containing organic compounds using group contribution methods. *Atmos. Environ.* **2002**, *36*, 1483−1498.
(48) Pankow, J. F. An absorption model of gas/particle partitioning of organic compounds in the atmosphere. *Atmos. Environ.* **1994**, *28* (2), 185−188.

Received for review February 7, 2007. Revised manuscript received June 20, 2007. Accepted June 20, 2007.

ES070314N